



# Enhancing the surface morphology for improved phase change mechanism by Sm doping in $\text{Ge}_2\text{Sb}_2\text{Te}_5$ thin films

Sanjay Kumar<sup>1</sup> · Vineet Sharma<sup>1</sup>

Received: 23 November 2020 / Accepted: 16 February 2021 / Published online: 27 February 2021  
© The Author(s), under exclusive licence to Springer-Verlag GmbH, DE part of Springer Nature 2021

## Abstract

The effect of doping of rare earth element Sm to  $\text{Ge}_2\text{Sb}_2\text{Te}_5$  (GST) phase change material (PCM) on the surface morphology in  $(\text{Ge}_2\text{Sb}_2\text{Te}_5)_{100-x}\text{Sm}_x$  ( $x=0, 0.6, 1.2$ ) thin films is investigated employing atomic force microscopy (AFM). The incorporation of Sm to GST thin films indicates composition dependent grain size distribution and surface roughness. The Sm doping impacts the nucleation dominated crystallization mechanism of GST phase change material. The root mean square roughness value in AFM micrographs of the thin films decreases with Sm content. The RMS roughness ( $R_q$ ) to average roughness ( $R_a$ ) ratio value 1.119 for  $x=0.6\%$  of Sm-doped GST thin films, points to the Gaussian distribution of grain sizes. The average grain size of  $(\text{Ge}_2\text{Sb}_2\text{Te}_5)_{100-x}\text{Sm}_x$  ( $x=0, 0.6, 1.2$ ) thin films shows a decrease on Sm incorporation which may be attributed to the compositional dependence of crystallization activation energy for phase change. Few sharp spikes on the thin film for  $x=1.2$  of Sm addition to GST suggest an increase in the hexagonal phase as compared to the fcc phase which may alter the mechanism of phase transition in these PCMs.

**Keywords** Surface morphology · Roughness · Crystallization · Nucleation · Growth · Average grain size

## 1 Introduction

The chalcogenide phase change materials exhibit rapid and reversible switching between the low and high resistance states. This resistive switching between the states has been used in phase change memory (PCM) devices for information storage [1]. The PCM devices have been considered as next-generation non-volatile memories. PCM devices can sandwich the performance gap between DRAMs and flash memories and will improve computing performance in many folds.

Among all the phase change materials, Ge–Sb–Te alloys are advantageous due to their fast switching speed and lower power consumption [2].  $\text{Ge}_2\text{Sb}_2\text{Te}_5$  (GST) in particular, has been considered as the novel material for this purpose [2]. The phase transition from amorphous to the crystalline phase of GST is the consequence of transformation of a fraction of GeTe tetrahedral units into defective octahedra

with the growth of 4-membered Ge–Te–Sb–Te rings in (200) direction resulting in the formation of rocksalt crystal structure, whereas all the 4a anionic sites are filled with Te and 4b cationic sites are occupied randomly by Ge, Sb and 20% of the vacancies [3]. The vacancies in the metastable fcc phase play a major role in the transition to hexagonal phase. The doping to vacancy sites is considered as the most preferred site for the stabilization of fcc phase; however, the dopants can accumulate at grain boundaries which may reduce the grain size [4, 5]. Researchers have done many efforts for improving the performance of GST by doping the foreign impurities like transition and the rare earth elements [6, 7]. The switching between the ordered and disordered states differs in the optical and electrical properties which are exploited for memory storage. The amorphous and crystalline states of the thin films of the phase change materials contrast in the structure and surface morphology. GST is a nucleation dominated phase change material [8]. For the nucleation dominated materials, the crystal grown process is relatively slower and many nuclei are formed in unit volume and the formation of nuclei is also exhibited during the growth process. These types of materials which show the nucleation dominated crystallization often form crystals of different sizes. The grain distribution and the presence of

✉ Vineet Sharma  
vineet.sharma@juit.ac.in

<sup>1</sup> Department of Physics and Materials Science, Jaypee University of Information Technology, Waknaghat, Solan, H.P. 173234, India

microcracks in the thermally evaporated thin films can be easily analyzed using the atomic force microscopy (AFM) which helps us to understand the crystallization and phase change in GST thin films. The crystallization causes shrinkage in the volume which may induce stressed phases in the thin film. The study of the surface morphology of thin films helps to distinguish the nucleation dominated and growth dominated mechanism in phase change materials.

In this study, the surface morphology of  $(\text{Ge}_2\text{Sb}_2\text{Te}_5)_{100-x}\text{Sm}_x$  ( $x=0, 0.6, 1.2$ ) thin films is analyzed using the AFM. The average grain size distribution is estimated which helps to understand the effect of Sm incorporation on the crystallization mechanism of GST phase change material. The root mean square roughness ( $R_q$ ), average roughness ( $R_a$ ), skewness ( $R_{sk}$ ) and kurtosis ( $R_{ku}$ ) are analyzed to understand the role of Sm addition to GST thin films to modify the surface morphology in altering the phase change mechanism.

## 2 Experimental

The melt quench technique is employed to prepare bulk samples of  $(\text{Ge}_2\text{Sb}_2\text{Te}_5)_{100-x}\text{Sm}_x$  ( $x=0, 0.6, 1.2$ ) by taking the 5 N pure elements Ge, Sb, Te and 99.9% pure Sm (Alfa Aesar) in their atomic weight percentage and sealing them in pre-cleaned quartz ampoules in high vacuum ( $\sim 10^{-6}$  mbar). The vacuum-sealed ampoules are kept inside the muffle furnace for 24 h with multistep heating maintaining the heating rate of 2 to 3 K/min. The multistep heating is done up to 1373 K, and then the red hot ampoules are melt quenched by dropping them into the ice-cooled water. The solid ingot is taken out from the ampoules by crushing gently. The ingot is crushed into the powdered form using mortar and pestle. The powdered sample is used as the evaporation source for the thin film deposition using the thermal evaporation unit (model no. HINDHIVAC 12A4D). The base pressure for film deposition is kept at  $\sim 10^{-6}$  mbar. The film thickness ( $\sim 1000$  nm) and the deposition rate (10 to 15 Å/s) of  $(\text{Ge}_2\text{Sb}_2\text{Te}_5)_{100-x}\text{Sm}_x$  ( $x=0, 0.6, 1.2$ ) thin films are maintained constant during the deposition. The rectangular microscopic glass slide ( $75 \times 25$  mm) is used as a substrate for the film deposition. The thin film obtained using this technique is used for structural analysis using the X-ray diffraction (XRD, PANalytical, X'pert) and the amorphous nature of the thin film is observed. The surface morphology of thin film is investigated using atomic force microscopy (AFM NTEGRA, NT-MDT) at room temperature and the AFM micrographs are taken at tapping mode. The surface roughness and grain distribution analysis of AFM images of  $(\text{Ge}_2\text{Sb}_2\text{Te}_5)_{100-x}\text{Sm}_x$  ( $x=0, 0.6, 1.2$ ) thin films are carried out using the NOVA Px 3.2.2 rev. 9252 software.

## 3 Results and discussion

The  $(\text{Ge}_2\text{Sb}_2\text{Te}_5)_{100-x}\text{Sm}_x$  ( $x=0, 0.6, 1.2$ ) thin films are analyzed using the X-ray diffraction for their structure. The XRD spectra of as deposited  $(\text{Ge}_2\text{Sb}_2\text{Te}_5)_{100-x}\text{Sm}_x$  thin films measured in Bragg–Brentano geometry using the Cu  $K\alpha$  X-ray source are shown in Fig. 1. The absence of any sharp peaks in the XRD spectra suggests the amorphous nature of as deposited  $(\text{Ge}_2\text{Sb}_2\text{Te}_5)_{100-x}\text{Sm}_x$  thin films.

Figure 2a–c shows the 3D AFM images of  $(\text{Ge}_2\text{Sb}_2\text{Te}_5)_{100-x}\text{Sm}_x$  ( $x=0, 0.6, 1.2$ ) thin films deposited on glass substrate. The crystallization mechanism of GST phase change material is nucleation dominated. In nucleation dominated crystallization process, the critical barrier energy for the formation of the nucleus is relatively lower in comparison with the crystal growth [9]. The nucleation dominated crystallization and surface morphology of high-resolution AFM micrographs ( $5 \times 5 \mu\text{m}$ ) of  $(\text{Ge}_2\text{Sb}_2\text{Te}_5)_{100-x}\text{Sm}_x$  ( $x=0, 0.6, 1.2$ ) thin films are studied.

The average roughness ( $R_a$ ) and root mean square roughness ( $R_q$ ) for  $(\text{Ge}_2\text{Sb}_2\text{Te}_5)_{100-x}\text{Sm}_x$  ( $x=0, 0.6, 1.2$ ) thin films are analyzed and summarized in Table 1. The  $R_q$  value signifies the standard deviation of the peak profile from the average roughness value. The  $R_a$  and  $R_q$  values are observed to decrease on Sm addition. The  $R_q$  to  $R_a$  ratio value signifies the statistical distribution of peak heights. For the Gaussian distribution of surface peak heights, the values of ratio  $R_q/R_a$  must be less than 1.25 [10], as analyzed from Figs. 2a, b for the samples  $x=0$  and  $x=0.6$ , respectively, signifying the Gaussian distribution of surface peak heights. But, for  $x=1.2$ , this ratio differs as observed from the Fig. 2c indicative of the deviation from Gaussian distribution. The skewness ( $R_{sk}$ ) represents the variation of surface peak profile

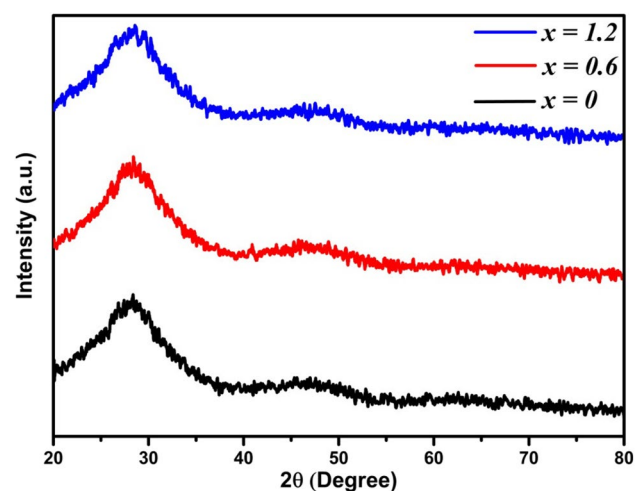
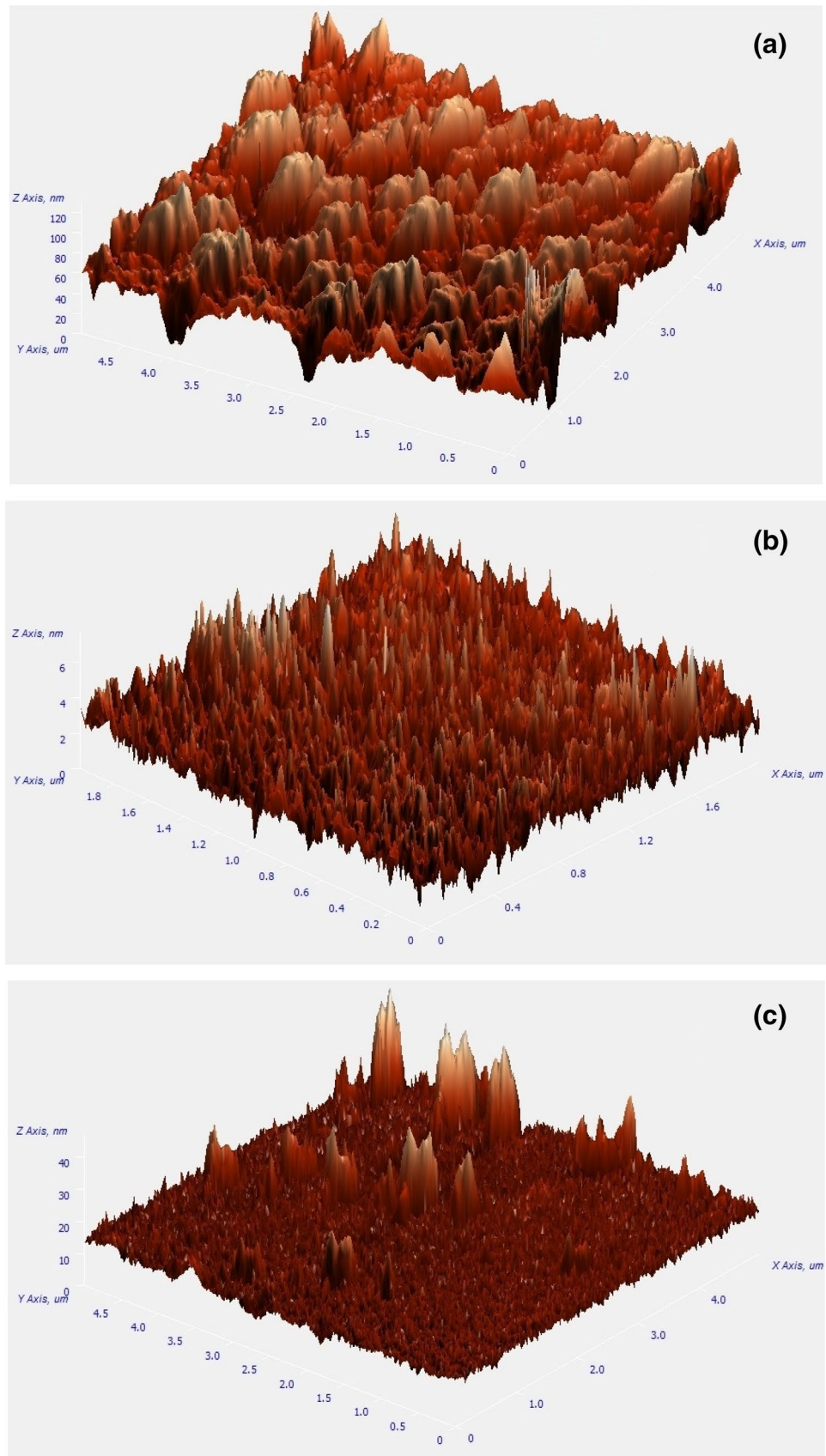


Fig. 1 The XRD spectra of  $(\text{Ge}_2\text{Sb}_2\text{Te}_5)_{100-x}\text{Sm}_x$  ( $x=0, 0.6, 1.2$ ) thin films

**Fig. 2** **a** 3D AFM image of  $(\text{Ge}_2\text{Sb}_2\text{Te}_5)_{100-x}\text{Sm}_x$  ( $x=0$ ) thin film. **b** 3D AFM image of  $(\text{Ge}_2\text{Sb}_2\text{Te}_5)_{100-x}\text{Sm}_x$  ( $x=0.6$ ) thin film. **c** 3D AFM image of  $(\text{Ge}_2\text{Sb}_2\text{Te}_5)_{100-x}\text{Sm}_x$  ( $x=1.2$ ) thin film



**Table 1** AFM roughness and average grain size parameters for  $(\text{Ge}_2\text{Sb}_2\text{Te}_5)_{100-x}\text{Sm}_x$  ( $x=0, 0.6, 1.2$ ) thin films

$x$	$R_q$ (nm)	$R_a$ (nm)	$R_q/R_a$	$R_{sk}$	$R_{ku}$	Average grain length (nm)	Average grain width (nm)	Aspect ratio	Mean value of average grain size (nm)
0	26.19	21.98	1.19	-0.962	2.959	38.5	17.08	2.236	23.84
0.6	0.62	0.52	1.19	0.119	2.342	34.2	15.3	2.203	22.70
1.2	2.76	1.73	1.59	1.999	13.349	27.7	12.6	2.140	18.50

about the mean line or plane. The  $R_{sk}$  value is negative for  $x=0$  which represents the dominance of the valley depths over the surface peak heights. The  $R_{sk}$  value increases from 0.119 for Sm content  $x=0.6$  and to 1.999 for  $x=1.2$ . The increase in skewness value (Table 1) is due to the increase in peak heights in comparison with the valley depths on Sm incorporation. The spiky and bumpy surfaces are analyzed using the evaluation of roughness kurtosis ( $R_{ku}$ ) parameter for  $(\text{Ge}_2\text{Sb}_2\text{Te}_5)_{100-x}\text{Sm}_x$  ( $x=0, 0.6, 1.2$ ) thin films. The  $R_{ku}$  value is less than 3 for bumpy surfaces and greater than 3 spiky surfaces [10]. The surface profile of GST thin films on Sm addition is observed to be bumpy for  $x=0$  and  $x=0.6$  and spiky for  $x=1.2$  (Table 1) as can be seen from the 3D AFM images illustrated in Fig. 2a–c.

Figure 3a–c shows the 2D AFM height images analyzed for grain boundary analysis for  $(\text{Ge}_2\text{Sb}_2\text{Te}_5)_{100-x}\text{Sm}_x$  thin films using the NOVA Px 3.2.2 rev. 9252 software. The average grain size histograms for Sm incorporated GST thin films are displayed in Fig. 4a–c. The Gaussian fitting for the average grain size histogram is performed and the Gaussian equation is displayed in Fig. 4a–c indicating the same. Figure 3a shows the formation of grains in clusters having irregular shapes with large voids in between the clusters. The value of aspect ratio greater than 2 (Table 1) indicates the formation of non-spherical grains for the undoped GST thin films ( $x=0$ ). For  $x=0$ , the Fig. 4a shows the average grain size histogram of the grains displayed in Fig. 3a with the mean value of 23.84 nm and the standard deviation of 17.22 nm. The large value of standard deviation is due to the nucleation dominated crystallization mechanism of GST phase change materials which displays the heterogeneous nucleation. The grain distribution image of AFM height image for  $x=0.6$  and  $x=1.2$  of Sm-doped GST thin films is shown in Fig. 3b, c, respectively. The average grain size is observed to decrease in Sm incorporation to GST thin films. Figure 4b, c illustrate the average grain size histogram for  $x=0.6$  and  $x=1.2$  of Sm-doped GST thin films, respectively.

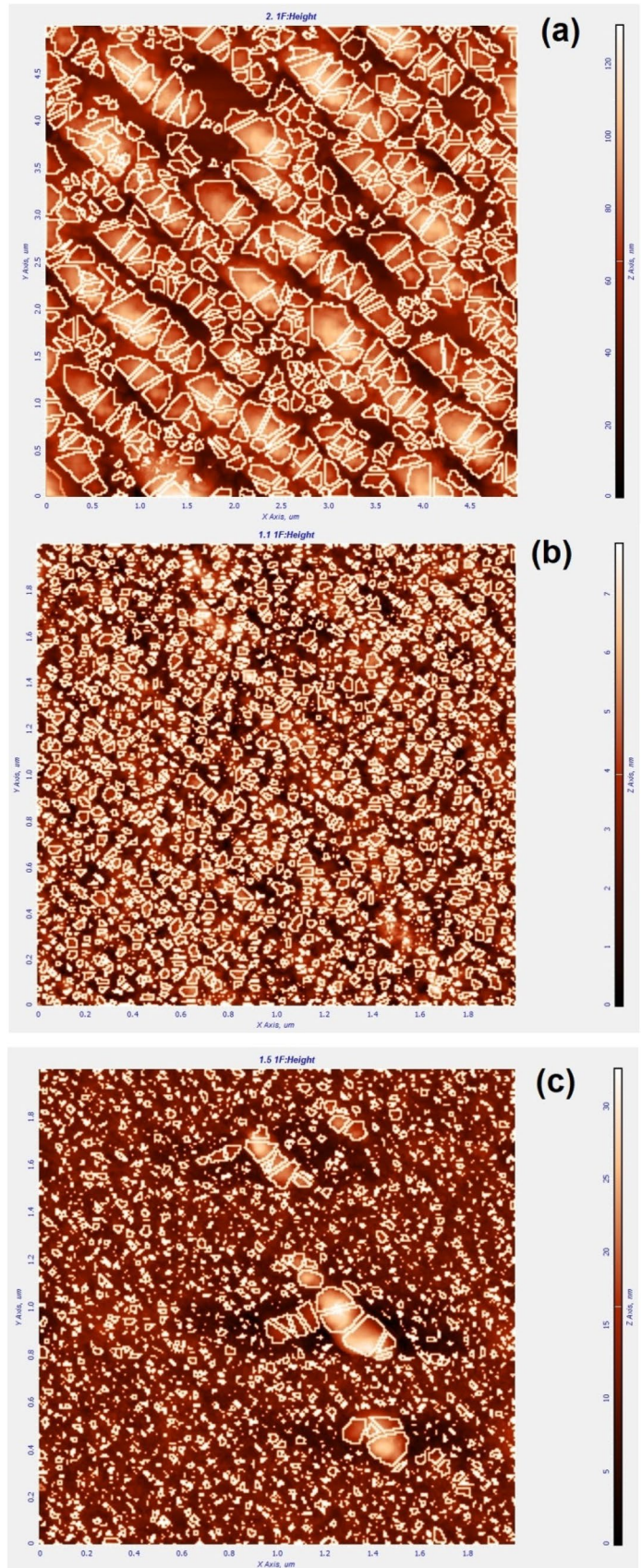
The local elastic behavior of the thin films may be observed employing AFM. The deflection of cantilever tip from the hard and the soft surface varies due to the large reflection of oscillation by harder surface and causing the large deflection in cantilever tip, while the soft surfaces absorb the oscillations and cause the smaller deflections

of cantilever tip. The color contrast in AFM height images signifies the deflection in the harder and the softer regions [11, 12]. The amorphous GST usually witnesses the crystallization process which consists of two steps. The amorphous phase may make transition from fcc to hexagonal phase. It is reported that the density of grains in fcc GST crystal structure is 6.8% larger than the amorphous GST due to the shrinking of GST in crystalline phase in comparison with their amorphous counterpart [13]. Generally, the nonuniform distribution of the grain size is due to the heterogeneous rate of nucleation leading to an increase in film roughness and the formation of bigger sized grains. The transition between fcc and hexagonal phases of GST plays a critical role in dictating the speed of phase change in GST phase change materials. The addition of rare earth element Sm in the present work modifies the process of this transition.

In the present study, the variation of average grain size with Sm content is analyzed. The decrease in average grain size and the aspect ratio with Sm incorporation manifests the decrease in the heterogeneous nucleation rate and the formation of nearly spherical grains on Sm incorporation. The RMS roughness values for the investigated films decrease due to the formation of homogeneous grain shapes on Sm incorporation to GST. However, few bright spikes are observed in 3D AFM image for the  $x=1.2$  of Sm incorporation which are nearly triangular, which may be due to the different grain growth rates in the cubic and hexagonal phases [3]. The cubic and hexagonal phases are found to coexist in Sm-doped GST thin films [14]. The Sm incorporation can improve the crystal growth rate in nucleation dominated [15] GST phase change materials. The formation of small-sized uniform grains along with few sharp spikes in the AFM micrograph of  $x=1.2$  of Sm-doped GST thin film may be due to the improvement in heterogeneous nucleation rate and alternation of crystallization kinetics [16] on Sm addition. The grain growth kinetics follows the general Arrhenius equation  $G^n = K_0 t \exp\left(-\frac{E_a}{RT}\right)$  where  $G$ ,  $n$ , and  $K_0$  are the average grain size, grain growth exponent and constant, respectively [17]. The value for  $n=2$  for the classical uniform grain growth process [18, 19]. The change in the value of average grain size with Sm content is utilized for the evaluation of change in activation energy ( $E_a$ ) with Sm



**Fig. 3.** 2D AFM height image simulated for grain boundaries using the NOVA Px 3.2.2 rev. 9252 software for **a**  $(\text{Ge}_2\text{Sb}_2\text{Te}_5)_{100-x}\text{Sm}_x$  ( $x=0$ ) thin film. **b**  $(\text{Ge}_2\text{Sb}_2\text{Te}_5)_{100-x}\text{Sm}_x$  ( $x=0.6$ ) thin film. **c**  $(\text{Ge}_2\text{Sb}_2\text{Te}_5)_{100-x}\text{Sm}_x$  ( $x=1.2$ ) thin film



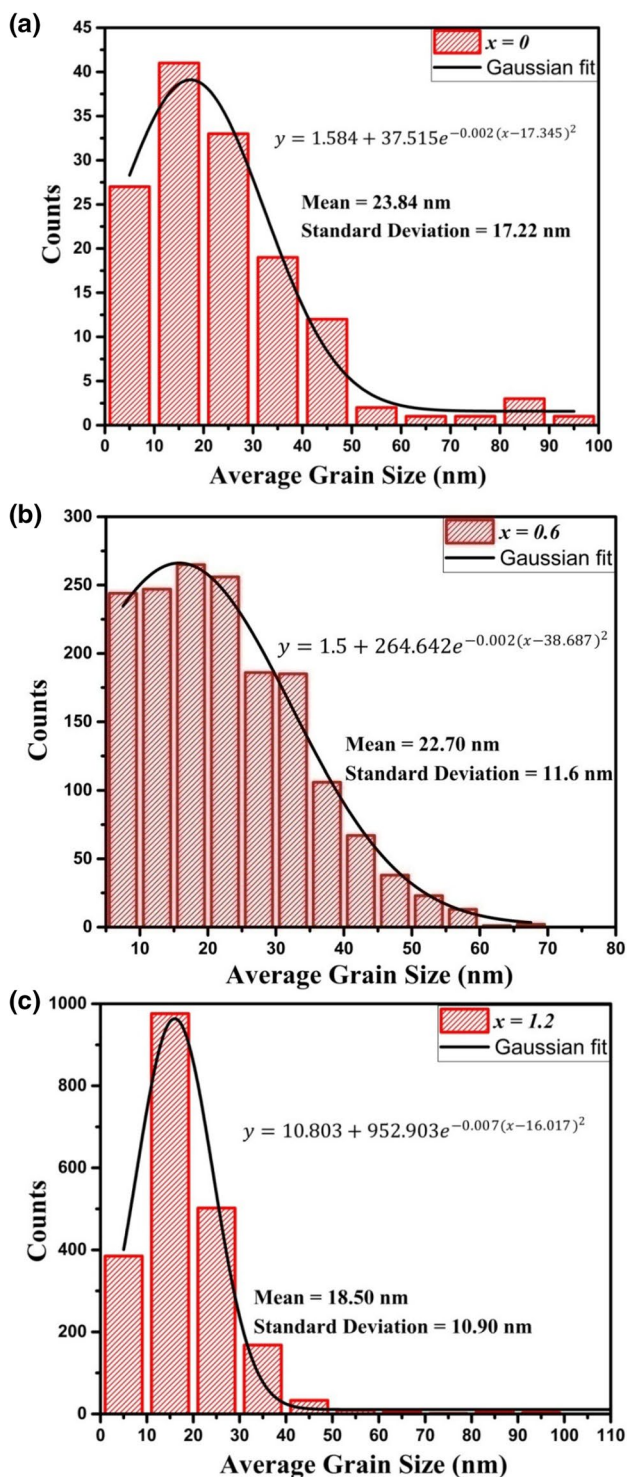


**Fig. 4** Average grain size histogram for  $(\text{Ge}_2\text{Sb}_2\text{Te}_5)_{100-x}\text{Sm}_x$  thin films **a** for  $x=0$ , **b** for  $x=0.6$  and **c** for  $x=1.2$

content using the equation  $\ln(G_0)^2 - \ln(G_1)^2 = \frac{-E_{a0} + E_{a1}}{RT}$  where  $G_0$  and  $G_1$  represent the average grain sizes at two different compositions and  $T$  is the room temperature, i.e.,

300 K. The difference ( $E_{a1} - E_{a0}$ ) of activation energies for 1.2% Sm-doped and the undoped GST is found to be 0.13 eV which signifies an increase in the activation energy by the same magnitude for the sample with 1.2% Sm doping. The grain size modification of GST thin films on Sm addition has broad significance in phase transition and reduces the activation energy of crystallization on phase change drastically.

## 4 Conclusion

The modification in the surface morphology of  $(\text{Ge}_2\text{Sb}_2\text{Te}_5)_{100-x}\text{Sm}_x$  ( $x=0, 0.6, 1.2$ ) thin films prepared by thermal evaporation technique is analyzed using AFM to analyze the effect of Sm content. The morphology of undoped sample  $x=0$  is observed to be bumpy with dominant valley depths over the peak height areas. The value of  $R_{ku}$  greater than 3 for  $x=1.2$  of Sm incorporation to GST indicates the spikes in the thin film suggesting the dominance of peak height over the valley depths. The value of  $R_q/R_a$  ratio close to 1.25 for  $x=0$  and  $x=0.6$  thin films suggests the Gaussian distribution of the average grain size. Few sharp spikes for  $x=1.2$  of Sm addition are observed on the film surface. The average grain size decreases from 23.84 to 18.50 nm on Sm incorporation to GST thin films. The surface roughness improves on Sm incorporation to GST as inferred from the decrease in standard deviation of average grain size. The uniformity of grain distribution also improves on Sm addition to GST thin films indicating a homogeneous rate of nucleation. The decrease in average grain size and surface roughness in GST thin films on Sm incorporation may improve the activation energy for crystallization of phase change materials for data storage applications.

**Acknowledgements** This work is financially supported by the Science and Engineering Research Board (SERB), Department of Science and Technology (DST) of India with project file no. EMR/2016/006094, dated 05th October 2017. SK is thankful to SERB-DST, New Delhi for providing financial support as JRF. The authors thank Prof. N. S. Negi, Department of Physics, Himachal Pradesh University Shimla, H.P. India for providing the AFM facility.

## References

1. B. Kersting, M. Salinga, Exploiting nanoscale effects in phase change memories. *Faraday Discuss.* **213**, 357–370 (2019)
2. W. Zhang, R. Mazzarello, M. Wuttig, E. Ma, Designing crystallization in phase-change materials for universal memory and neuro-inspired computing. *Nat. Rev. Mater.* **4**(3), 150–168 (2019)
3. W. Zhang, H.S. Jeong, S.A. Song, Martensitic transformation in  $\text{Ge}_2\text{Sb}_2\text{Te}_5$  alloy. *Adv. Eng. Mater.* **10**(1–2), 67–72 (2008)

4. K.H. Song, S.W. Kim, J.H. Seo, H.Y. Lee, Characteristics of amorphous Ag<sub>0.1</sub> (Ge<sub>2</sub> Sb<sub>2</sub> Te<sub>5</sub>) 0.9 thin film and its ultrafast crystallization. *J. Appl. Phys.* **104**(10), 7 (2008)
5. W.-X. Song et al., Improving the performance of phase-change memory by grain refinement. *J. Appl. Phys.* **128**(7), 075101 (2020)
6. Y. Chen et al., Electrical properties and structural transition of Ge<sub>2</sub> Sb<sub>2</sub> Te<sub>5</sub> adjusted by rare-earth element Gd for nonvolatile phase-change memory. *J. Appl. Phys.* **124**(14), 145107 (2018)
7. H. Zou, Y. Hu, X. Zhu, Z. Song, Simultaneously high thermal stability and ultra-fast phase change speed based on samarium-doped antimony thin films. *RSC Adv.* **7**(49), 31110–31114 (2017)
8. J.L. Bosse, I. Grishin, B.D. Huey, O.V. Kolosov, Nanomechanical morphology of amorphous, transition, and crystalline domains in phase change memory thin films. *Appl. Surf. Sci.* **314**, 151–157 (2014)
9. S. Privitera, C. Bongiorno, E. Rimini, R. Zonca, Crystal nucleation and growth processes in Ge<sub>2</sub>Sb<sub>2</sub>Te<sub>5</sub>. *Appl. Phys. Lett.* **84**(22), 4448–4450 (2004)
10. B. Rajesh Kumar, T. Subba Rao, AFM studies on surface morphology, topography and texture of nanostructured zinc aluminum oxide thin films. *Dig. J. Nanomater. Biostruct.* **7**(4), 1881–1889 (2012)
11. R.W. Carpick, M. Salmeron, Scratching the surface: Fundamental investigations of tribology with atomic force microscopy. *Chem. Rev.* **97**(4), 1163–1194 (1997)
12. K.E. Strawhecker, E. Manias, AFM of poly(vinyl alcohol) crystals next to an inorganic surface. *Macromolecules* **34**(24), 8475–8482 (2001)
13. Y. Wu, K. Liu, D. Li, Y. Guo, S. Pan, In situ AFM and Raman spectroscopy study of the crystallization behavior of Ge<sub>2</sub> Sb<sub>2</sub> Te<sub>5</sub> films at different temperature. *Appl. Surf. Sci.* **258**(4), 1619–1623 (2011)
14. S. Privitera, C. Garozzo, A. Alberti, L. Perniola, B. De Salvo, Mixed phase Ge<sub>2</sub>Sb<sub>2</sub>Te<sub>5</sub> thin films with temperature independent resistivity. *AIP Adv.* **3**(1), 012105 (2013)
15. Q. Yin, L. Chen, The mechanism of texture formation during crystallization process of Ge<sub>2</sub>Sb<sub>2</sub>Te<sub>5</sub> thin films. *Cryst. Res. Technol.* **52**(2), 1600243 (2017)
16. S. Song, Z. Song, L. Wu, B. Liu, S. Feng, Stress reduction and performance improvement of phase change memory cell by using Ge<sub>2</sub>Sb<sub>2</sub>Te<sub>5</sub>-TaOx composite films. *J. Appl. Phys.* **109**(3), 034503 (2011)
17. A.S. Demirkiran, S. Yilmaz, U. Sen, Grain growth kinetics of glass-ceramic produced from power plant fly ash. *Int. J. Appl. Ceram. Technol.* **8**(6), 1444–1450 (2011)
18. S. Lombardo, E. Rimini, M.G. Grimaldi, S. Privitera, Amorphous-fcc transition in Ge<sub>2</sub>Sb<sub>2</sub>Te<sub>5</sub>. *Microelectron. Eng.* **87**(3), 294–300 (2010)
19. K.N. Zhu, Q. Ruan, A. Godfrey, The kinetics of grain growth in near-micrometre grain size copper produced by spark plasma sintering. *IOP Conf. Ser. Mater. Sci. Eng.* **89**(1), 012060 (2015)

**Publisher's Note** Springer Nature remains neutral with regard to jurisdictional claims in published maps and institutional affiliations.